Scattering of O_2 from a graphite surface

2012 J. Phys.: Condens. Matter 24 104010

(http://iopscience.iop.org/0953-8984/24/10/104010)

IOP PUBLISHING JOURNAL OF PHYSICS: CONDENSED MATTER
J. Phys.: Condens. Matter **24** (2012) 104010 (9pp) doi:10.1088/0953-8984/24/10/104010

Scattering of O_2 from a graphite surface

W W Hayes[1,2], Junepyo Oh[3], Takahiro Kondo[3], Keitaro Arakawa[3], Yoshihiko Saito[3], Junji Nakamura[3] and J R Manson[2]

[1] Physical Sciences Department, Greenville Technical College, Greenville, SC 29606, USA
[2] Department of Physics and Astronomy, Clemson University, Clemson, SC 29634, USA
[3] Graduate School of Pure and Applied Science, University of Tsukuba, 1-1-1 Tennoudai, Tsukuba, Ibaraki 305-8573, Japan

E-mail: Wayne.Hayes@gvltec.edu and jmanson@clemson.edu

Received 1 July 2011, in final form 15 August 2011
Published 21 February 2012
Online at stacks.iop.org/JPhysCM/24/104010

Abstract
Recently an extensive series of measurements has been presented for the angular distributions of oxygen molecules scattered from a graphite surface. Incident translational energies ranged from 291 to 614 meV with surface temperatures from 150 to 500 K. The measurements were taken with a fixed angle of 90° between the source beam and the detector and the angular distributions consisted of a single broad peak with the most probable intensity located at an angle slightly larger than the 45° specular position. Analysis with the hard cubes model for atom–surface scattering indicated that the scattering is primarily a single collision event with a surface having a collective effective mass much larger than a single carbon atom. Limited analysis with a classical diatomic molecular scattering theory was also presented. In this paper a more complete analysis using the classical diatomic molecular scattering theory is presented. The energy and temperature dependence of the observed angular distributions are well described as single collision events with a surface having an effective mass of 1.8 carbon graphite rings. In agreement with the earlier analysis and with other experiments, this suggests a large cooperative response of the carbon atoms in the outermost graphene layer.

1. Introduction

The interaction of graphitic surfaces with molecular oxygen is an interesting problem that is of fundamental interest to such widely different applications as understanding the phenomenon of burning to the reduction reaction in fuel cells. Thus it is of interest to study the interaction of oxygen molecules with carbon surfaces under conditions in which the collision energy and surface temperature are well defined.

Recently a series of measurements for well defined supersonic molecular beams of oxygen scattering from clean and ordered graphite surfaces has been published [1]. These experiments reported the scattered angular distributions resulting from a highly collimated and nearly monoenergetic incident beam of O_2 scattering from the surface of highly oriented pyrolytic graphite. The experiments were carried out with a fixed source–detector geometry in which the angle between the incident beam and the detector direction was held at an angle of 90°. The incident energies ranged between 291 and 614 meV and the surface temperatures were from 150 to 500 K. For each energy and temperature combination the angular distribution intensities were reported as a function of final detector angle θ_f relative to the surface normal, which means that at each final angle the incident angle was given by $\theta_i = \pi/2 - \theta_f$.

As functions of θ_f the angular distributions consisted of single broad peaks with a maximum (the most probable intensity) occurring at an angle slightly larger than the specular position of 90°. As the incident energy is increased the peaks increase somewhat in maximum intensity and become narrower. As a function of increasing surface temperature, the maximum intensity decreases and the width increases. This behavior is indicative of a scattering collision that can be described by classical mechanics where the collision involves large energy transfers and exchange of large numbers of phonons or electronic excitations [2, 3].

These data were originally analyzed with the hard cubes model of Logan and Stickney [4] which describes the classical interaction of an atomic particle with a surface having an effective mass under the rather stringent condition of conservation of momentum parallel to the surface. This analysis concluded that the predominant scattering process

was the O_2 molecules making a single collision with a surface whose effective mass is approximately nine times heavier than a single carbon atom, indicating a collective effect. The data were also partially analyzed with a classical rigid molecular scattering theory which supported the basic conclusions arising from the hard cubes model.

This paper presents a more complete analysis of the O_2/graphite angular distributions using classical rigid molecular scattering theory. Molecular oxygen presents an interesting test of the nature of the collision interaction because it is substantially heavier than the mass of a single carbon atom. If the collision is viewed as a single oxygen molecule colliding with a single carbon atom only forward scattering would occur, implying that the incoming oxygen would continue to penetrate through the surface and suffer multiple collisions with other carbon atoms. However, the fact that the majority of the incoming beam intensity is scattered back away from the surface with little time delay indicates that the collision is a collective mechanism in which the oxygen collides with many carbon atoms having a collective mass greater than that of the oxygen molecule. Similar conclusions have been drawn for the collision of Xe atoms colliding with a graphite surface [5, 6].

The results of the present analysis using classical diatomic scattering theory gives a very good description of both the temperature and incident translational energy dependence of the observed angular distributions. The explanation of the data is significantly better than that provided by the hard cubes model. The results confirm the conclusion that the collision is a collective interaction with a number of carbon atoms in the outer graphene layer having an effective mass significantly larger than that of the oxygen molecule.

2. Experiment

The apparatus consists of five stainless-steel chambers, each independently pumped to ultrahigh vacuum (UHV), as has been described elsewhere [7, 8]. The supersonic O_2 beam is created by free-jet expansion of a gas of 10% oxygen seeded in He. The free-jet expansion is through a pinhole nozzle of diameter 0.05 mm and is then skimmed using a conical skimmer. The stagnation pressure in the nozzle is controlled by a commercial gas regulator from 1 to 100 atm. The translational energy E_i^T of the molecular beam is controlled by heating the nozzle from a temperature of 300–700 K within a temperature fluctuation of ± 0.1 K. The nozzle temperature is monitored by a type-K (chromel/alumel) thermocouple spot-welded at the edge of the nozzle near the pinhole. The incident beam of molecules is reflected from graphite in the scattering chamber and the scattered particles are detected by a quadrupole mass spectrometer (ULVAC MSQ-400) in the detector chamber. The energy spread $\Delta E_i/E_i$ of the incident beam is less than 20%. The detailed profiles of the molecular beam were measured by time-of-flight methods.

The sample of highly oriented pyrolytic graphite (HOPG, ZYA-grade, Panasonic, 12 mm × 12 mm × 1.5 mm) was cleaved in air by adhesive tape and then placed into the UHV chamber. The HOPG sample was mounted on a sample holder which can be cooled down to 90 K by a cryogenic refrigerator head (Iwatani CryoMini S050) and can be heated by infrared radiation from a hot W filament placed close to the back side of the HOPG sample. The surface temperature of the HOPG was measured by a type-K thermocouple attached on the edge of the sample surface by a Ta clamp. Prior to the experiment, the HOPG sample was annealed at 800 K in UHV for 5 min in order to clean the surface.

After heat treatment, angular intensity distribution measurements of the oxygen molecules scattered from the graphite surface are carried out by rotating the sample along the axis perpendicular to the beam line with an accuracy of $\pm 0.1°$. Both incident and scattering angles are defined with respect to the surface normal direction and the sum of the incident and scattering angles was fixed at 90°. For the purposes of comparing measured data with theoretical calculations, it should be noted that the detector is velocity dependent with the detector sensitivity proportional to the inverse of the final molecular speed.

3. Theory

The theory used for the calculations carried out in this paper was developed previously as a part of a mixed quantum-classical theory describing the scattering of small molecules from a surface, in which both the internal vibrational and rotational modes of the molecule were included [9, 10]. This theory was developed starting from the basic principles of a classical theory of scattering of atomic projectiles from surfaces originally proposed by Brako and Newns. The atomic projectile theory has been quite useful in explaining a large body of experimental measurements, and it is of interest to start by presenting that here because it will provide a useful comparison to the full rigid molecular scattering theory used here. For the case of an atomic projectile of mass m scattering from a smooth, flat surface whose only corrugations are due to small thermal vibrations of the underlying atomic cores the differential reflection coefficient $dR(\mathbf{p}_f, \mathbf{p}_i)/d\Omega_f\, dE_f^T$ is given by [11–13]

$$\frac{dR(\mathbf{p}_f, \mathbf{p}_i)}{d\Omega_f\, dE_f^T} \propto \frac{|\mathbf{p}_f|}{p_{iz}} |\tau_{fi}|^2 \left(\frac{\pi}{k_B T_S \Delta E_0^T}\right)^{3/2} \times \exp\left\{-\frac{(E_f^T - E_i^T + \Delta E_0^T)^2 + 2v_R^2 \mathbf{P}^2}{4k_B T_S \Delta E_0^T}\right\}, \quad (1)$$

where p_{iz} is the surface normal component of the incident momentum, T_S is the temperature, k_B is Boltzmann's constant, the binary recoil energy for translational motion is $\Delta E_0^T = (\mathbf{p}_f - \mathbf{p}_i)^2/2M_S$ with M_S the target substrate mass, $\mathbf{P}$ is the parallel component of the scattering vector $\mathbf{p} = \mathbf{p}_f - \mathbf{p}_i$, and τ_{fi} is a transition matrix determined from the interaction potential. The incident translational energy is $E_i^T = \mathbf{p}_i^2/2m$, with a similar expression for the final energy E_f^T. v_R is a parameter having dimension of speed that is completely determined by the phonon spectral density at the classical

turning point, but which is usually treated as a parameter as is the case here [11, 12].

The form factor τ_{fi} is the transition matrix of the interaction potential taken between the initial incoming state and the final outgoing state. An approximation that has been useful in describing atom–surface scattering is the Born approximation matrix element of the interaction potential taken in the hard repulsive wall limit which gives

$$\tau_{fi} = \frac{2p_{iz}p_{fz}}{m}. \tag{2}$$

This expression for the form factor has been used for numerous calculations of atomic and molecular surface scattering and has provided good explanations of both measured angular distributions and energy resolved spectra [3].

The extension of equation (1) to the case of a rigid diatomic molecule with incident translational momentum $\mathbf{p}_i$ and angular momentum $\mathbf{l}_i$ scattering into the state denoted by $\mathbf{p}_f$ and $\mathbf{l}_f$ is the following:

$$\begin{aligned}\frac{dR(\mathbf{p}_f,\mathbf{l}_f;\mathbf{p}_i,\mathbf{l}_i)}{d\Omega_f\,dE_f^T} \propto{}& \frac{|\mathbf{p}_f|}{p_{iz}}|\tau_{fi}|^2\left(\frac{\pi}{\Delta E_0^T k_B T_S}\right)\\ &\times\left(\frac{\pi}{\Delta E_0^R k_B T_S}\right)^{1/2}\left(\frac{\pi}{(\Delta E_0^T+\Delta E_0^R)k_B T_S}\right)^{1/2}\\ &\times\exp\left[-\frac{2\mathbf{P}^2 v_R^2}{4\Delta E_0^T k_B T_S}\right]\exp\left[-\frac{2l_z^2\omega_R^2}{4\Delta E_0^R k_B T_S}\right]\\ &\times\exp\left[-\frac{(E_f^T-E_i^T+E_f^R-E_i^R+\Delta E_0^T+\Delta E_0^R)^2}{4(\Delta E_0^T+\Delta E_0^R)k_B T_S}\right].\end{aligned} \tag{3}$$

where E_f^R and E_i^R are the final and initial rotational energies of the molecular projectile. The quantity l_z is the component of the angular momentum scattering vector $\mathbf{l} = \mathbf{l}_f - \mathbf{l}_i$ normal to the surface. The rotational recoil energy is given by

$$E_0^R = \frac{l_x^2}{2I_{xx}} + \frac{l_y^2}{2I_{yy}} + \frac{l_z^2}{2I_{zz}}, \tag{4}$$

where the I_{jj} are the principle components of the moment of inertia tensor of the surface. The constant ω_R plays a similar role for rotational transfers as the weighted average of parallel phonon velocities v_R in equation (1). Both of these quantities can be computed if the complete dynamical structure function of the surface is known. For the purpose of this work, these quantities will be treated as parameters. In fact, for all calculations shown in section 4 below, ω_R was chosen to be around 10^{-12} s^{-1}. For values of ω_R this small it has negligible effect on the results of calculations even if it is changed by as much as an order of magnitude.

For the experiments of [1] considered here, no information was obtained on the rotational state of the O_2 molecules as only angular distribution intensity spectra were measured. This means that in order to compare with the experimental data equation (3) must be averaged over initial projectile angular momenta and summed over all final angular momenta.

The angular distribution is given by the integral over all final energies of the differential reflection coefficient, but the detector efficiency correction must be taken into account in this process. In these experiments the detector is a density detector which means that the detector efficiency decreases in inverse proportion to the final translational momentum. Furthermore, the detector is located at a fixed angle of $\theta_{SD} = 90°$ with respect to the incident beam. The incident angle θ_i and final angle θ_f are related by $\theta_f + \theta_i = \theta_{SD}$ which means that the in-plane angular distributions can be regarded as a function of the single angle θ_f. Explicitly, this means that the angular distributions reported in section 4 below are given by

$$\frac{dR(\theta_f)}{d\Omega_f} = \int_0^\infty \frac{1}{\sqrt{E_f^T}}\frac{dR}{d\Omega_f\,dE_f^T}\,dE_f^T \tag{5}$$

where $dR/d\Omega_f\,dE_f^T$ has been averaged over initial angular momentum and summed over final angular momentum of the projectile molecules.

There are several parameters that remained fixed for all calculations presented in this paper. In all cases the incident beam of O_2 molecules was given an initial rotational energy of 2.6 meV corresponding to a rotational temperature of about 30 K. Although the incident rotational temperature was not measured, this estimate is consistent with the known fact that molecular jet beams are rotationally cold. The value of v_R is chosen to be 3000 m s^{-1} which is consistent with values chosen for other molecule–surface scattering calculations that have been carried out.

The principal moments of the moment of inertia tensor I are normally expected to be those of a surface molecule in the case of a molecular target. However, if the projectile molecules are large and strike more than one surface molecule simultaneously, then I is expected to become an effective moment of inertia, larger than that of a single molecule. In the case of monatomic solids, an effective surface molecule consisting of two or more surface atoms must be chosen. For the calculations considered here a value of $I_{jj} = 3.99 \times 10^{-46}$ kg m^2 was used. This corresponds approximately to that of a single six-carbon atom graphite ring taken with respect to an axis through the plane of the ring. The calculated results do not depend strongly on the choice of the value of the effective moment of inertia.

4. Calculated results

The angular distribution intensity spectra for six different surface temperatures ranging from 150 to 500 K are shown as a function of final scattering angle θ_f in figure 1. All of these data were taken for a fixed incident translational energy of 291 meV, and as mentioned before the incident and final angles are held at the fixed source–detector angle $\theta_{SD} = 90°$, thus each final angle corresponds to a different incident angle. The solid curves in figure 1 are the rigid diatomic calculations derived from equation (3). These calculations are carried out for an effective surface mass M_S equal to that of 1.8 carbon rings (129.6 amu). This value for the effective surface mass is determined by matching the most probable final angle

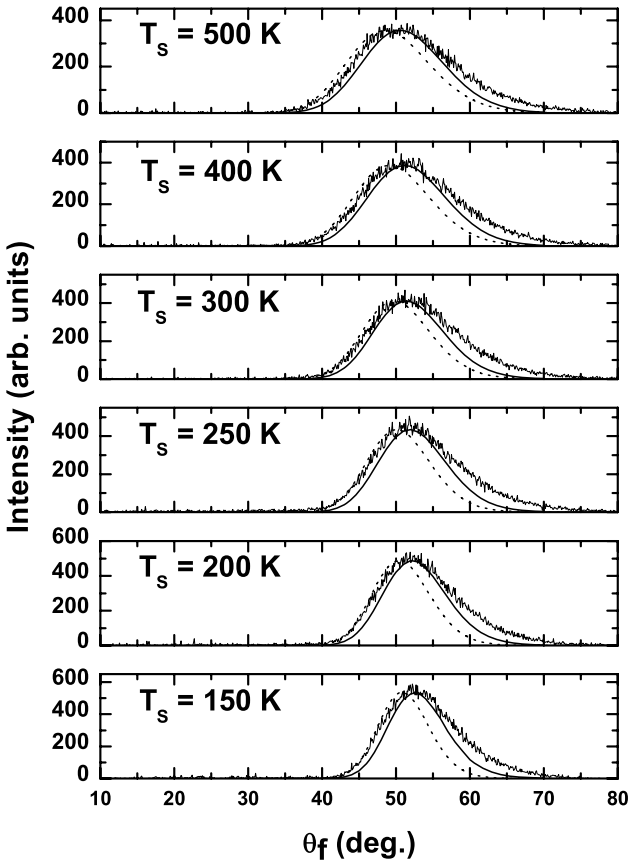

Figure 1. Angular distribution intensity spectra for scattering of O_2 from graphite taken with a fixed source–detector angle $\theta_{SD} = 90°$ and for incident translational energy $E_i^T = 291$ meV shown as a function of final scattering angle θ_f. The surface temperature T_S ranges from 150 to 500 K as marked. The solid curve is the rigid diatomic calculation and the dotted curve is the pseudo-atomic calculation, both with an effective surface mass equal to 1.8 carbon rings.

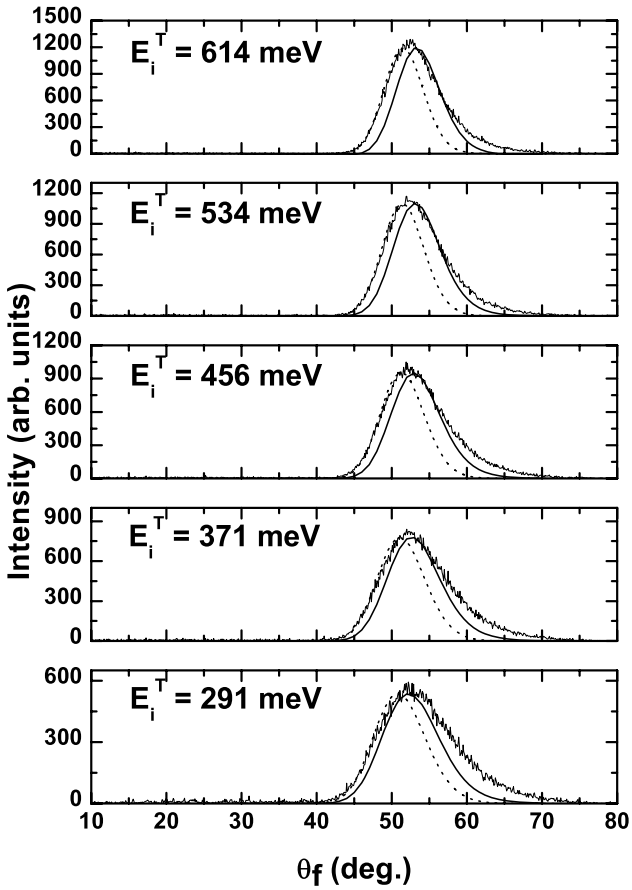

Figure 2. Angular distribution intensity spectra similar to figure 1 except for a fixed surface temperature $T_S = 150$ K and incident translational energies ranging from 291 to 614 meV as marked.

(the peak position in the angular distributions) to that of the experimental data over all surface temperatures and incident energies measured. The calculations are relatively sensitive to the value of the effective mass, and changing this mass by the mass of a single carbon atom will shift the most probable final angle by as much as 2°. The need for an effective mass much larger than that of a single carbon atom in atomic and molecular scattering from graphite has been recognized previously, and points to collective scattering from a large number of surface carbon atoms. This collective effect has been recognized for Xe atom scattering from graphite where the single scattering collective mechanism was called a 'trampoline' effect, since the majority of the collective carbon atoms appeared to come from the outermost graphene layer [5, 6]. A single scattering event with a large effective mass was necessary to interpret Ar scattering from graphite [15], and the present data were also analyzed with a hard cubes model which required an effective mass of approximately 108 amu (1.5 carbon rings).

The dotted curves also shown in figure 1 are, for comparison, a pseudo-atomic calculation of the angular distributions using the atom scattering differential reflection coefficient of equation (1). In this case the pseudo-atomic projectile mass is taken to be the same as that of an oxygen molecule, and the effective surface mass is the same 1.8 carbon rings as for the rigid diatomic calculation. It is seen that while the rigid diatomic calculations match the experimental data and the peak position rather well, the pseudo-atomic calculation peaks at an angle several degrees closer to the specular position. However, both calculated curves indicate that the scattering process is a single collision event with a collective surface.

Figure 2 is similar to figure 1 except it shows the dependence of the angular distributions on incident translational energy rather than the surface temperature. All five graphs in figure 2 are for the fixed temperature of 150 K while the incident energy ranges from 291 to 614 meV. As in figure 1 the rigid diatomic calculations for the same effective mass shown by the solid curves explain the experimental data reasonably well at all energies. The pseudo-atomic calculations are again shifted somewhat toward the specular.

The reasonably good explanation of the angular distribution data shown in the calculated curves in figures 1 and 2 are consistent with a description of the scattering process as a single collision event with a collective surface. However, it is of interest to examine the agreement in more detail by considering the temperature and energy dependence

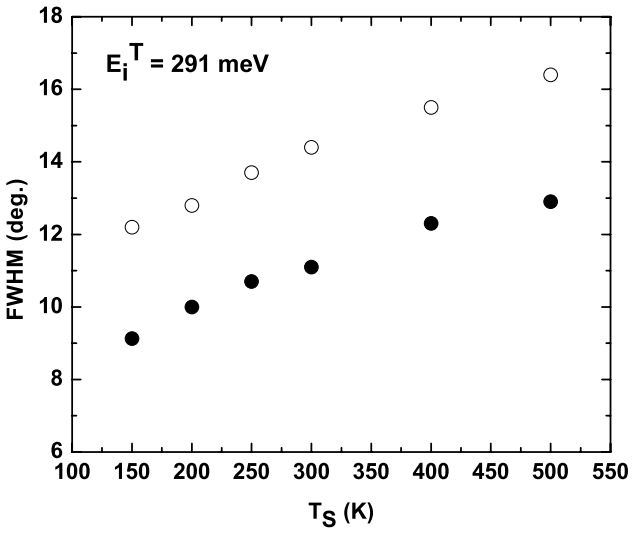

Figure 3. FWHM as a function of surface temperature T_S. The incident translational energy is 291 meV. The open circles are the data taken from figure 1 and the filled circles are the present rigid molecular theory calculations.

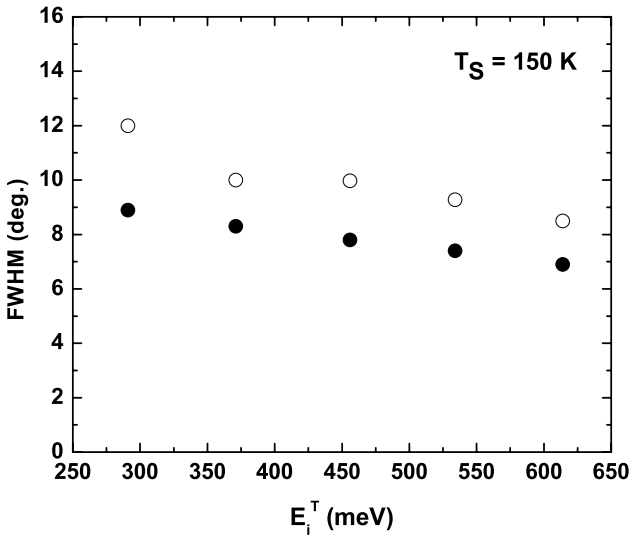

Figure 4. FWHM as a function of incident translational energy E_i^T at the fixed surface temperature of 150 K. The open circles are the data taken from figure 2 and the filled circles are the present rigid molecular theory calculations.

of the various characteristics of the angular distribution spectra. This is done in the following, where the full width at half maximum (FWHM), the most probable final angle, and the most probable intensity are viewed as functions of the temperature and incident translational energy.

Figure 3 shows the temperature dependence of the FWHM of the angular distributions measured in units of degrees. The open circles are the experimental data taken from figure 1 with a fixed incident energy of 291 meV. The data show a small increase of about 5° over the measured temperature range. The calculations shown as filled circles have a similar temperature dependence with nearly the same slope as the data, but produce an FWHM that is about three degrees smaller than the experimental values at all temperatures.

The increase in FWHM with surface temperature is consistent with the differential coefficient of equation (3) which predicts that the energy resolved spectra should have widths that increase as $\sqrt{T_S}$. Figure 3 shows that this increasing, positive slope, behavior persists even after integrating the differential reflection coefficient over all final energies to obtain the angular distribution.

The fact that the measured data give FWHMs that are larger than the calculated values by a temperature independent constant value is indicative of other, temperature independent mechanisms that may be coming into play in the collision process. Primary among other possible mechanisms would be scattering from surface defects as has been proposed previously [1, 14, 15].

The incident translational energy dependence of the FWHM is shown in figure 4. Again, the experimental data taken from figure 2 are shown as open circles and the calculations are filled circles. In contrast to the dependence of the FWHM on T_S, its dependence on incident energy exhibits a small decrease of about 3° over the range of energies investigated. Also as in figure 3 the calculations give a very good qualitative description of the experimentally observed behavior, exhibiting a very similar decreasing slope, but with the calculated points falling below the experiment by a nearly energy independent value of roughly 2°. Similarly, this indicates the presence of an energy independent mechanism, not included in the calculations, that increases the widths, and a likely source is also scattering from impurities.

It is interesting to note that this decrease of the FWHM of the angular distributions is not immediately evident in the behavior of the differential reflection coefficient. In fact the energy resolved diatomic differential reflection coefficient of equation (3), as well as the simpler atomic expression of equation (1), exhibits FWHMs that increase with incident energy when viewed as functions of final translational energy. The reason for this is that the FWHM behavior in equation (3) is governed primarily by the arguments of the Gaussian-like exponentials. In these arguments the translational recoil ΔE_0^T is always found multiplied by the temperature T_S. For the initial conditions of relatively large incident translational energies, such as found here, the translational recoil is very nearly proportional to the incident translational energy [3]. Thus the temperature and energy dependence of the differential reflection coefficient are similar. However, when the differential reflection coefficient is summed over the final energies in order to obtain an angular distribution, the calculations show a clear decrease of the FWHM with increasing incident translational energy in agreement with the experimental observations.

Figures 5 and 6 show the most probable final angle (or peak position) of the angular distributions as a function of temperature and incident translational energy, respectively. In both cases the most probable final angle is remarkably stable as a function of both T_S and E_i^T and the calculations, which agree well with the data, support this. As a function of T_S it is seen in figure 6 that there is a small (about 2°) decrease of the

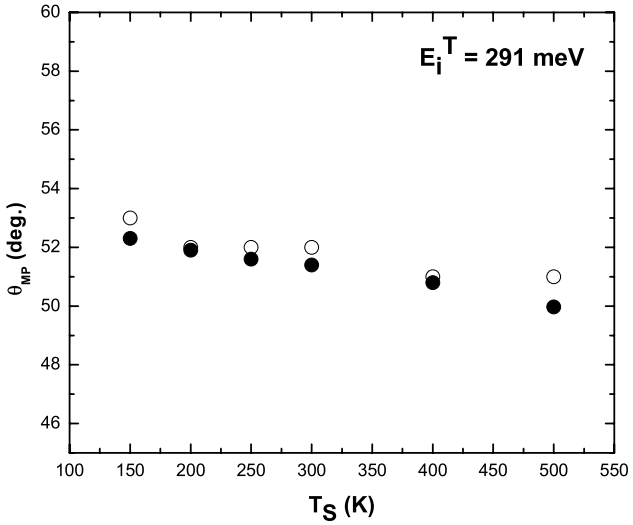

Figure 5. Most probable final angular position as a function of temperature for a fixed incident translational energy of 291 meV. Experimental points are open circles and calculations with the rigid molecular theory are filled circles.

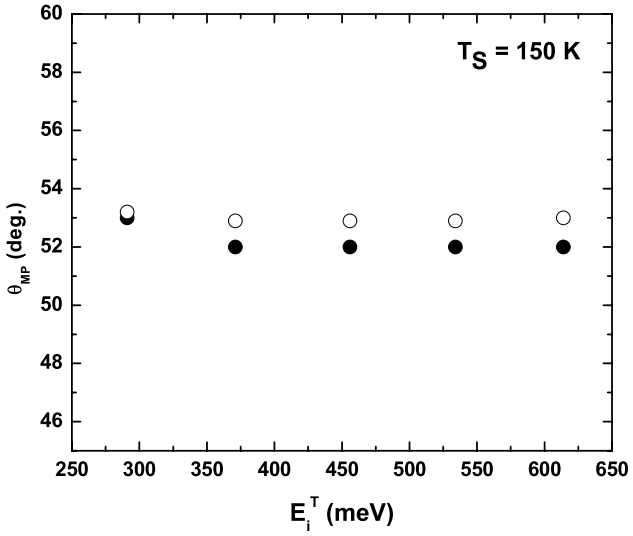

Figure 6. Most probable final angular position as a function of incident translational energy. The temperature is 150 K, experimental points are open circles and calculations are filled circles.

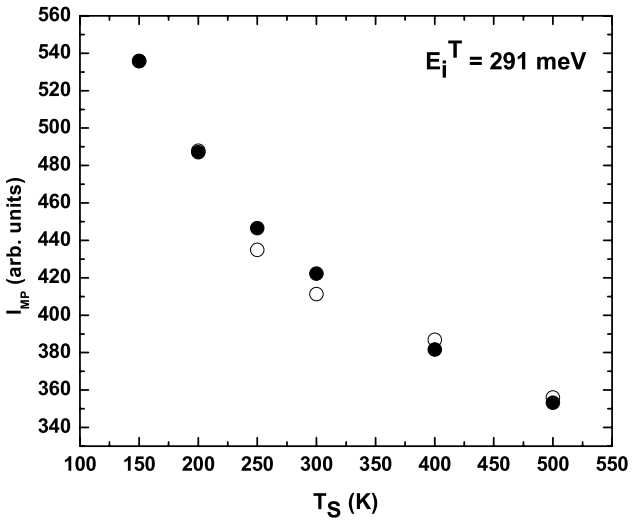

Figure 7. Most probable final intensity as a function of surface temperature T_S for an incident translational energy of 291 meV. The data, taken from figure 1 are shown as open circles. Rigid molecular theory calculations are shown as filled circles. At the two lowest temperatures the theory and data values are nearly identical and hence their points are indistinguishable.

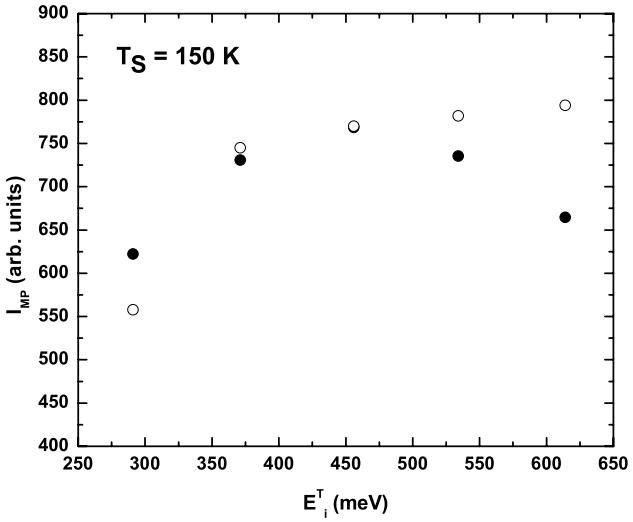

Figure 8. Most probable final intensity as a function of incident translational energy with $T_S = 150$ K. The data points, corrected for incident flux intensity, are shown as open circles. Rigid molecular theory calculations are shown as filled circles.

peak position (shift toward the specular angle of 45°) over the temperature range from 150 to 500 K. As a function of E_i^T the peak position is essentially unchanged over the entire energy range of about 300 meV.

Figures 7 and 8 show the most probable intensity of the angular distribution spectra (the peak intensity) as a function of T_S and E_i^T, respectively. As a function of temperature figure 7 shows a very distinct and monotonic decrease in maximum intensity. This decrease is implied by the inverse powers of T_S in the differential reflection coefficient of equation (3) and this decreasing behavior persists in the integrated angular distributions. The physical interpretation of this decrease of peak intensity is that since the width of the angular distribution increases with T_S the maximum intensity must simultaneously decrease in order to assure that the number of scattered particles remains constant (i.e. to assure unitarity of the scattering process).

Obtaining good relative intensities for different incident translational energies such as shown in figure 8 presents an experimental problem that does not exist when simply changing the temperature of the target sample while leaving the characteristics of the incident beam unchanged. When the incident translational energy of the beam is changed this is accomplished either by changing the temperature of the beam stagnation chamber or by changing the ratio of the seeding rare gas. In either case, this changes the incident

flux. Furthermore, at each incident energy the pressure in the stagnation chamber is adjusted to maximize the energy resolution of the jet beam. Thus, when obtaining experimental scattered intensities as a function of incident beam energy a correction must be made at each energy to account for the change in incident flux. The standard way to do this is to correct the incident flux according to the relative pressure in the sample chamber compared to that in the sample chamber when the incident beam is turned off. The data points shown in figure 8 are corrected data. The corrected data are the most probable intensity divided by a correction factor, and the correction factor at each incident energy is the relative pressure in the sample chamber divided by the pressure in the sample chamber when the beam is turned off. The data in figure 8 show that the dependence of the most probable intensity in incident energy increases rapidly at low energy and then less rapidly at higher energy. The calculations agree well with the initial increasing behavior, but at larger energies decrease again.

The final results to be discussed here are estimates of the typical translational and rotational energy transfers occurring at points across the range of final angles in the angular distributions. Since the experiment did not measure energy transfers directly these must be inferred from analysis with a model. The hard cubes model, which assumes that the momentum parallel to the surface is conserved, gives an approximation to the translational energy loss. This was used in [1] to estimate that the average energy loss to the surface at all incident translational energies was about 30–41% of the incident translational energy.

The theory used here based on the rigid molecular differential reflection coefficient of equation (3) provides detailed information on the energy transfer, and perhaps the most revealing measure is the translational energy resolved intensity, as exhibited in the solid curves in each panel of figure 9. This presents the calculated scattered intensity as a function of final translational energy E_f^T for the angle positioned at the most probable final angle, and the panels are calculated at each of the different incident translational energies of figure 2 as marked. The surface temperature is 150 K. Each of these curves, viewed as a function of final energy, is Gaussian-like and symmetric about the most probable final energy. This implies that the most probable final translational energy is a good measure of the energy transferred since it will be essentially the same as the average final translational energy taken for that same fixed final angle.

For comparison, also shown in figure 9 as dotted curves are the corresponding calculations for the pseudo-atomic model of equation (1) evaluated for the same angles and final translational energies. For all incident energies, the pseudo-atomic calculation peaks at a slightly higher final translational energy than the rigid molecular calculation. This is the expected behavior since the rigid molecular model can exchange energy to both phonon and rotational modes, thus it is not surprising that its final translational energy is lower than that of the pseudo-atomic calculation.

At all incident energies shown in figure 9 the differential reflection coefficient consists of a single peak as described

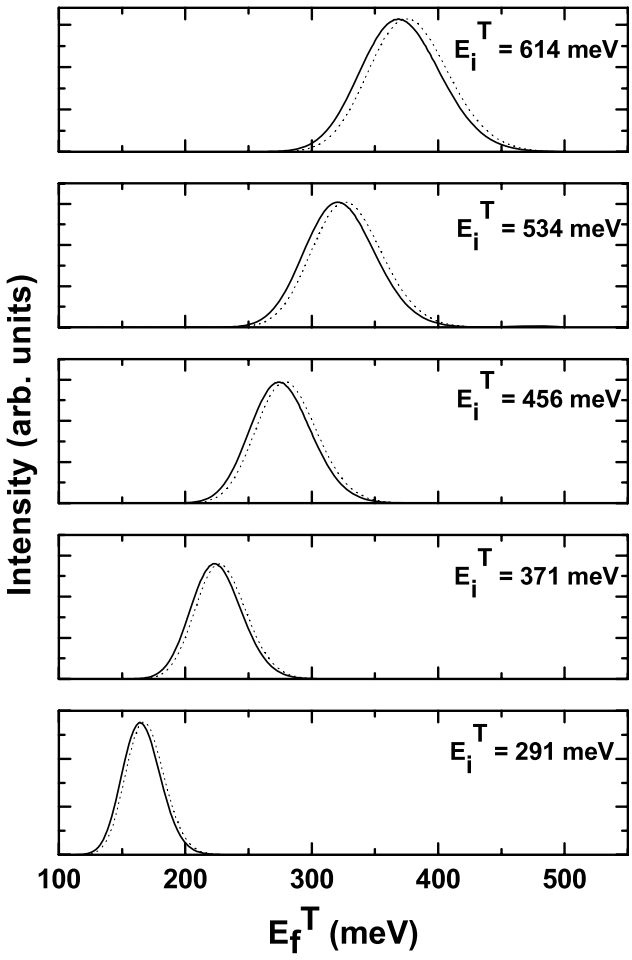

Figure 9. Solid curves: rigid molecular theory differential reflection coefficient as a function of final translational energy for all incident translational energies shown in figure 2 as marked, evaluated at the most probable final angle of the angular distribution spectrum for each incident energy. The surface temperature is 150 K. The dotted curves show the pseudo-atomic calculation evaluated at the same final translational conditions and for the same effective mass of 1.8 carbon rings.

above. The most probable final translational energy (peak energy) for all incident energies except the lowest is at very nearly 60% of the incident translational energy, and for the lowest energy of 291 meV it is very nearly the same value at 56%. These values are consistent with the upper limit of the range of translational energy losses estimated earlier with the hard cubes model [1] The most probable final energy calculated from equation (3) at final angles smaller than the most probable final angle, i.e. in the direction closer to specular, are monotonically larger than the values shown in figure 9. Similarly, for larger final angles the most probable final energy becomes smaller. Another measure of the typical final scattered translational energy would be the average final energy calculated over the entire range of non-negligible scattered intensities. Such calculations of the average final translational energy are very close to the most probable final energies shown in figure 9.

Calculations of the final rotational energy distributions for the rigid molecular theory of equation (3) predict

that the O_2 molecules are scattered from the surface with their rotational energy enhanced. For example, for the final scattering conditions corresponding to the most probable final translational energies shown in figure 9, the average final rotational energies range from 64.5 meV for the incident energy $E_i = 291$ to 79.8 meV for the higher incident energy $E_i = 614$ meV. Since the incident rotational energy in all cases is only 2.6 meV this corresponds to average rotational energy transfers ranging from 62 meV at low energy up to 77 meV at high incident translational energy. It is interesting to compare these rotational energy transfers to the differences in final translational energies as exhibited between the molecular and pseudo-atomic predictions in figure 9. There, the difference in most probable final translational energies (i.e. the difference in peak positions) ranges from about 4 to 7 meV as the incident translational energy is increased from 291 to 614 meV. This implies, based on energy conservation arguments, that the large transfer of energy to rotational states in the molecular O_2 collision event comes at the expense of less energy transferred to the surface phonons as compared to that for a corresponding pseudo-atomic projectile.

5. Discussion and conclusions

This paper presents a complete analysis of recently measured angular distribution intensities for the scattering of O_2 molecules from the surface of graphite. The analysis uses the classical theory of scattering from a surface of a rigid rotating molecule given in equation (3) which describes energy and momentum transfer with the surface in both rotational and translational degrees of freedom.

The experimental data consist of an extensive collection of total intensity angular distribution spectra as a function of final scattering angle, taken with a fixed angle between the beam source and the detector. The angular distributions were measured over a range of surface temperatures from 150 to 500 K and for a range of incident translational energies from 291 to 614 meV [1].

When initially presented, these data were analyzed with the hard cubes model, which accounts for energy transfers in the translational degrees of freedom and uses the severe approximation that momentum parallel to the surface remains unchanged in the scattering process. This analysis produced reasonable qualitative agreement with much of the experimental data and led to the conclusion that the O_2/graphite scattering consisted primarily of single collision events, but with an effective mass of approximately 108 amu (nine carbon atoms) which implied a collective collision involving a number of carbon atoms.

The present analysis with a rigid molecular scattering theory that allows for energy and momentum transfer in both translational and rotational degrees of freedom gives a much more quantitative description of the data, as is evident in the direct comparisons with the angular distributions shown in figures 1 and 2. Further more detailed analysis of the data is shown in figures 3 through 8 which consider the temperature and translational energy dependence of the FWHM, the most probable final angle, and the most probable intensity of the angular distributions. All of these quantities were well described by the rigid diatomic theory of equation (3) when used with a surface collective mass of 1.8 graphite rings (approximately 130 amu or 11 carbon atoms).

The good agreement between theory and experiment obtained here again confirms the initial conclusion that the scattering process is predominantly a single collision event with a collective mass on the surface. This conclusion is in accord with experiments using heavy rare gases scattering from graphite, notably Ar and Xe [15, 5, 6]. In fact, for the scattering of Xe from graphite a comparison of the data with molecular dynamics calculations of the collision process indicated that the majority of the carbon atoms involved in the collective mass were in the tightly bound outermost graphene layer, hence they called this collective effect 'trampoline' scattering [6].

Because the differential reflection coefficient of equation (3) gives a complete description of energy and momentum transfer in both translational and rotational degrees of freedom it can be used to estimate typical energy transfers in the present experiments. Although rotational energy exchange was not measured here, such transfers have been considered in previous work [16]. In this present work, estimates of the average rotational energy transfers to the scattered molecules are roughly 12–20% of the incident translational energies. A good measure of the typical translational energy transfer is the most probable final energy calculated at the most probable angle (peak angle) of the measured angular distributions. Such calculations are presented in figure 9 where it is seen that the typical final energy after a collision is about 60% of the incident translational energy. Calculated average final translational energies, averaged over the entire angular distribution produce similar values.

The good agreement between theory and experiment achieved here not only confirms the initial conclusion that the collision is a collective process with a number of surface atoms, but it also implies that the basic elements of the molecule–surface collision event between O_2 and graphite appear to be embodied in the differential reflection coefficient of equation (3). This indicates that the molecule–surface scattering theory of equation (3) is a useful model for describing molecular scattering collisions from surfaces under classical conditions where multiple quanta of energy are transferred. It should be a useful guide for predicting the translational and rotational momentum spectra of scattered molecules as functions of the experimentally controllable initial parameters such as temperature, mass, molecular species, translational energy and rotational energy.

References

[1] Oh J, Kondo T, Arakawa K, Saito Y, Hayes W W, Manson J R and Nakamura J 2011 *J. Phys. Chem.* A **115** 7089
[2] Barker J A and Auerbach D J 1985 *Faraday Discuss.* **80** 277
[3] Manson J R 2008 *Surface Dynamics* (*Handbook of Surface Science* vol 3) ed E Hasselbrink and B Lundqvist (Amsterdam: Elsevier)
[4] Logan R M and Stickney R E 1966 *J. Chem. Phys.* **44** 195

[5] Watanabe Y, Yamaguchi H, Hashinokuchi M, Sawabe K, Maruyama S, Matsumoto Y and Shobatake K 2005 *Chem. Phys. Lett.* **413** 331
[6] Watanabe Y, Yamaguchi H, Hashinokuchi M, Sawabe K, Maruyama S, Matsumoto Y and Shobatake K 2006 *Eur. Phys. J.* D **38** 103
[7] Kondo T, Kato H S, Yamada T, Yamamoto S and Kawai M 2006 *Eur. Phys. J.* D **38** 129
[8] Kondo T, Kato H S, Bonn M and Kawai M 2007 *J. Chem. Phys.* **127** 094703
[9] Iftimia I and Manson J R 2001 *Phys. Rev. Lett.* **87** 093201
[10] Iftimia I and Manson J R 2002 *Phys. Rev.* B **65** 125412
[11] Brako R and Newns D M 1982 *Phys. Rev. Lett.* **48** 1859
Brako R and Newns D M 1982 *Surf. Sci.* **117** 422
[12] Meyer H-D and Levine R D 1984 *Chem. Phys.* **85** 189
[13] Manson J R 1991 *Phys. Rev.* B **43** 6924
[14] Oh J, Kondo T, Hatake D, Honma Y, Arakawa K, Machida T and Nakamura J 2010 *J. Phys.: Condens. Matter* **22** 304008
[15] Yamada Y *et al* 2010 *J. Phys.: Condens. Matter* **22** 304010
[16] Ambaye H and Manson J R 2006 *J. Chem. Phys.* **125** 084717